Electronic Supplementary Material (ESI) for Environmental Science: Nano.

Towards the development of Safer by Design TiO_2-based photocatalytic paint: impacts and performances

A. Rosset[a*], V. Bartolomei[a], J. Laisney[b], N. Shandilya[c], H. Voisin[c], J. Morin[d], I. Michaud-Soret[b], I. Capron[c], H. Wortham[d], G. Brochard[e], V. Bergé[e], M. Carriere[f], F. Dussert[f], O. Le Bihan[g], C. Dutouquet[g], A. Benayad[a], D. Truffier-Boutry[a], S. Clavaguera[a], S. Artous[a*]

Table of contents:

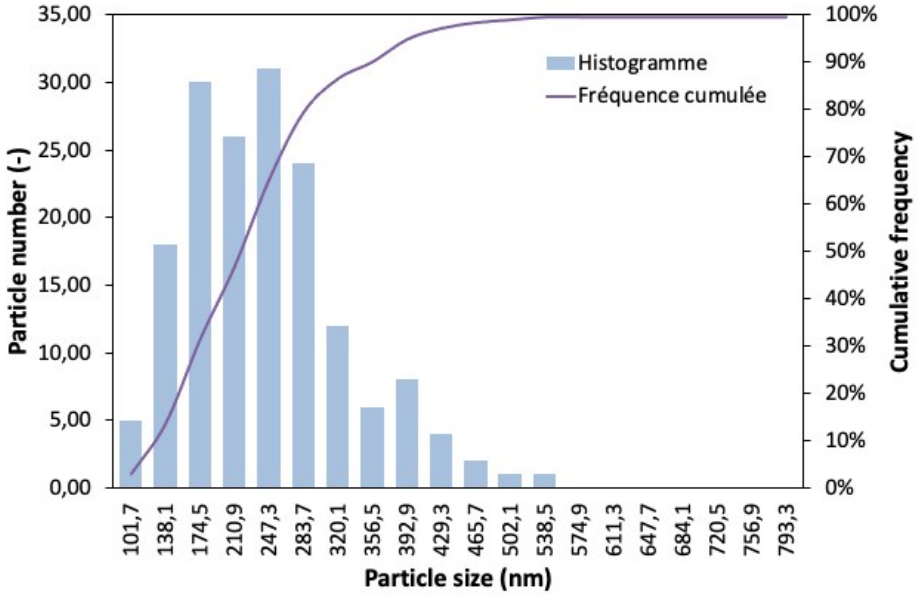

Fig. S1: Size distribution of microsized TiO_2 used in paint

The particles size distribution was based on the determination of the minimum Feret diameter of 237 nm particles base on 168 particles obtained by SEM, Hitachi S-5500, Japan.

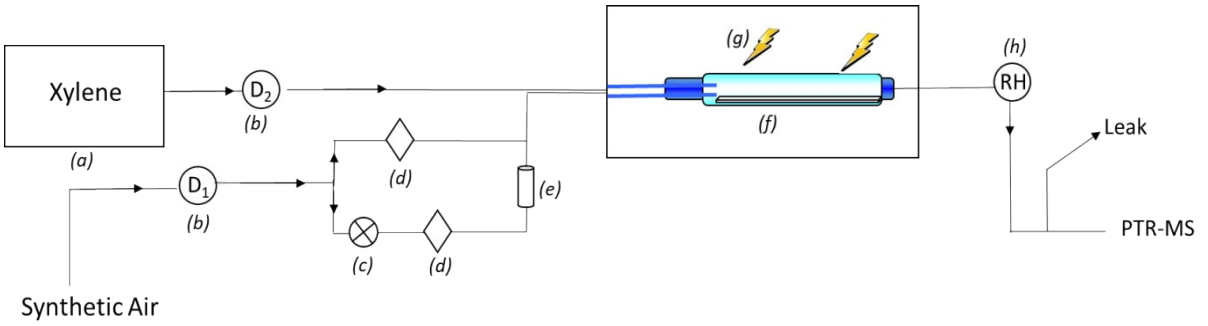

Fig. S2: Experimental set up for the measurement of VOCs elimination capacity or emission fluxes of photocatalytic paints. Permeation oven (a), mass flow controller (b), on/off valve (c), needle valve (d), relative humidity system (e), reactor + glass paint (f), UV-lamps (g), RH probe + hygrometer (f)

Text. S1: Photocatalytic efficiency: *m*-xylene generation and PTR-MS conditions

Gaseous *m*-xylene was generated using a sealed permeation cell and a gas phase generator (PUL 200, Saint Chamas, France). The sealed permeation cell consisting of a Teflon tube (perfluoroalkoxy, 4.0*6.4 mm, 8 cm long) filled with pure liquid m-xylene (Sigma Aldrich, > 99.5%) was used to generate gaseous xylene. This cell was placed in the oven chamber of the gas phase generator with a temperature of 60 °C. At the exit of the event, a constant flow of 10 sccm of gaseous *m*-xylene was allowed to enter in the movable injector. A sheath synthetic air flow of 190 sccm was added in the flow tube reactor to dilute m-xylene and obtained a concentration of 50 ppb of *m*-xylene.

The *m*-xylene mixing ratio was monitored in real time by a HS-PTR-MS by following its protonated molecular peak (m/z 107). This HS-PTR-MS high time resolution (10 s) allows us to measure rapid changes in gas phase concentration. The drift tube temperature was fixed at 333 K, the drift voltage at 500 V and the pressure at 2.02 mbar. These parameters corresponded to the E/N value of 124 Townsend.

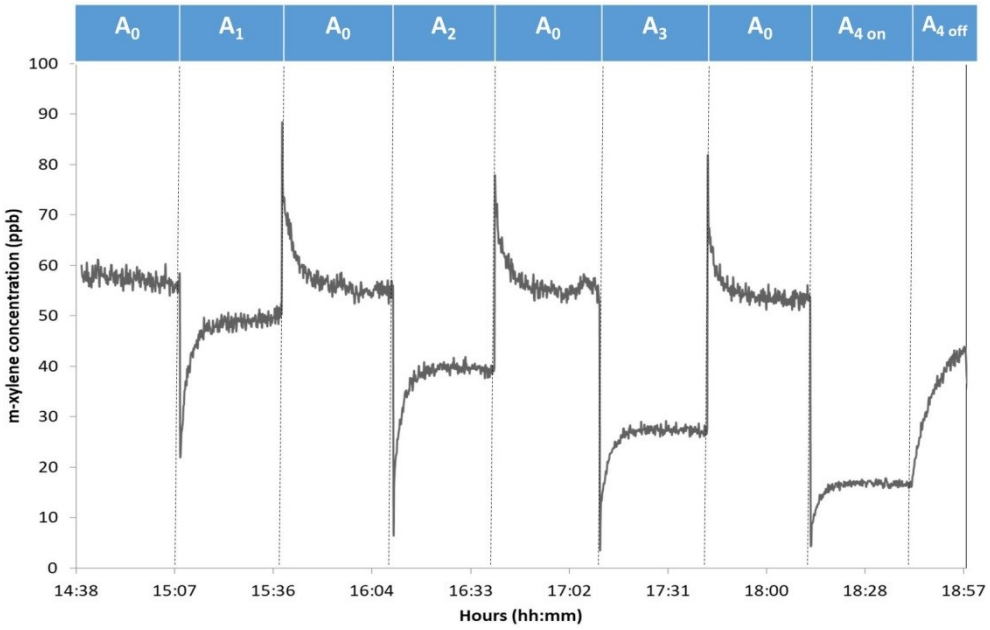

Fig. S3: Typical experiment of *m*-xylene light intensity: 8.8 W m^{-2}, Temperature: 298 K, RH: 40%, photocatalytic paint: P3 after 1000 hours of exposure to artificial weathering, initial mixing ratio of *m*-xylene: 55 ppb

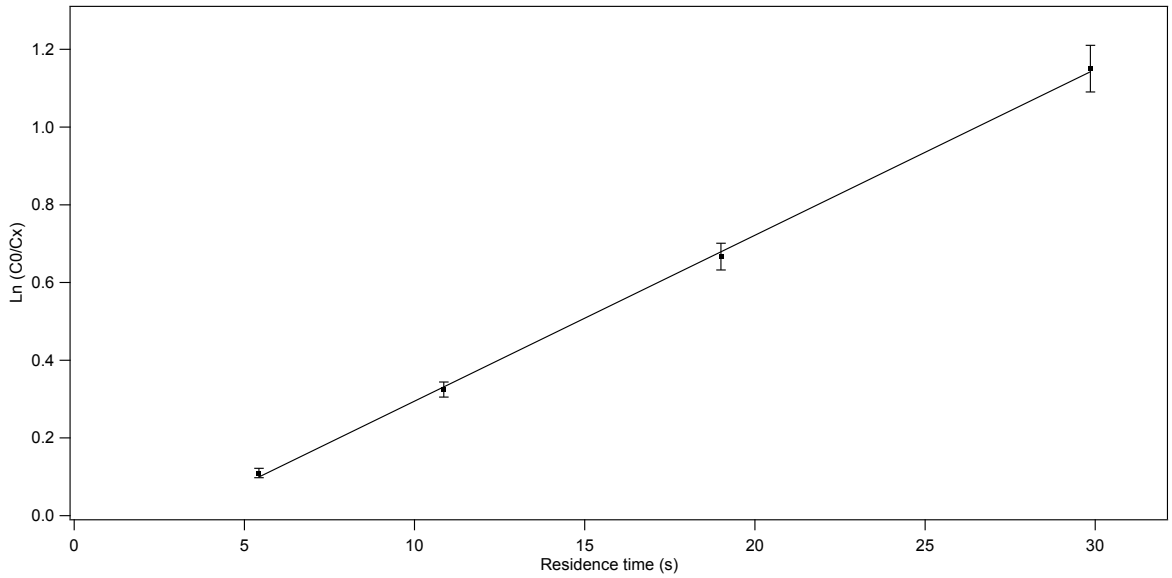

Fig. S4: Loss of gas phase *m*-xylene as a function of exposure time to a photocatalytic paint P3 under UV irradiation, after 1000 hours of exposure to artificial weathering, light intensity: 8.8 W m^{-2}, Temperature: 298 K, RH: 40%. Error bars are the propagation errors

X-Ray Diffraction.

The crystalline structural of commercial TiO_2 NPs wasinvestigated by X-Ray Diffraction (XRD) using a Bruker-advance diffractometer, USA,in geometry q-2q with Cu-Kαsource (λ = 1.5406 Å) and LynxEyelinear detector. The diffractogram was collected at 2θ in the range of 22° to 78° with 0.02° step.q-2q patterns were achieved in order to identify the various crystallographic phases and measure their lattice parameters. The positions of the diffraction peaks were in good agreement with the Powder Diffraction Standards data (JCPDS, no. 21-1272) corresponding to the anatase structure of TiO_2. The main peaks were identified as (101), (112), (200), (105), (211), (204), (220) and (215) reflection plane of anatase TiO_2, which corresponds to the diffraction angles at 2θ = 25.23°, 38.46°, 47.89°, 53.77°, 54.89°, 62.51°, 70.05° and 74.83°.

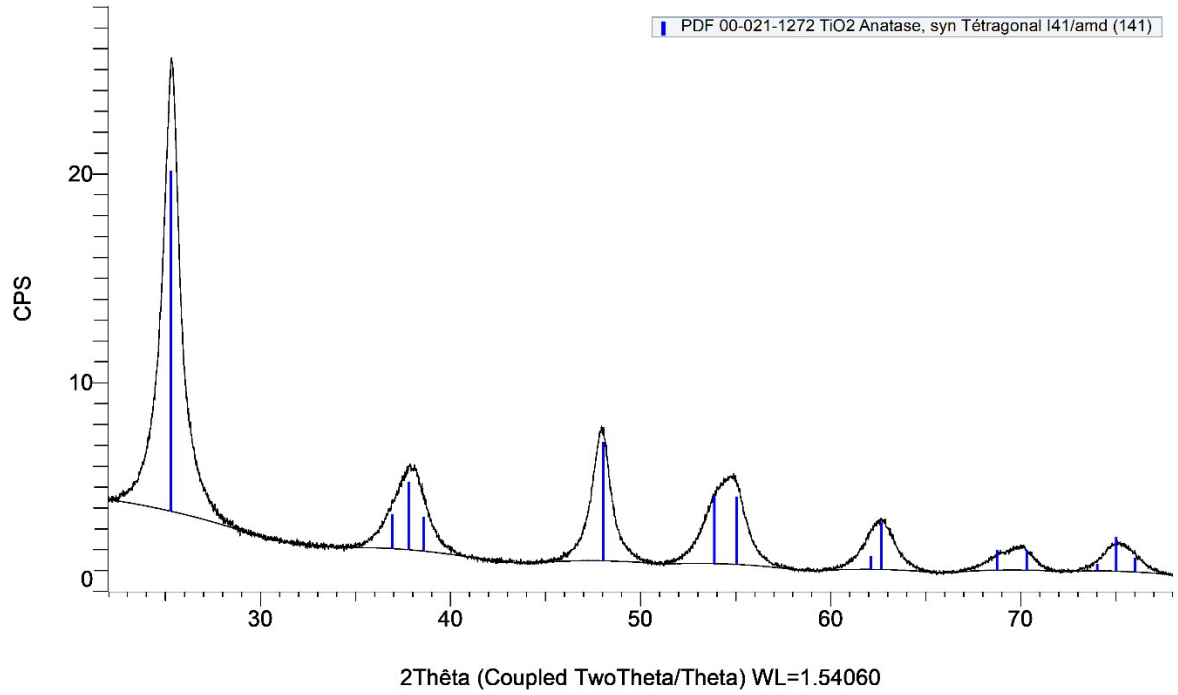

Fig. S5: XRD spectra of commercial TiO_2 nanoparticles used in paint

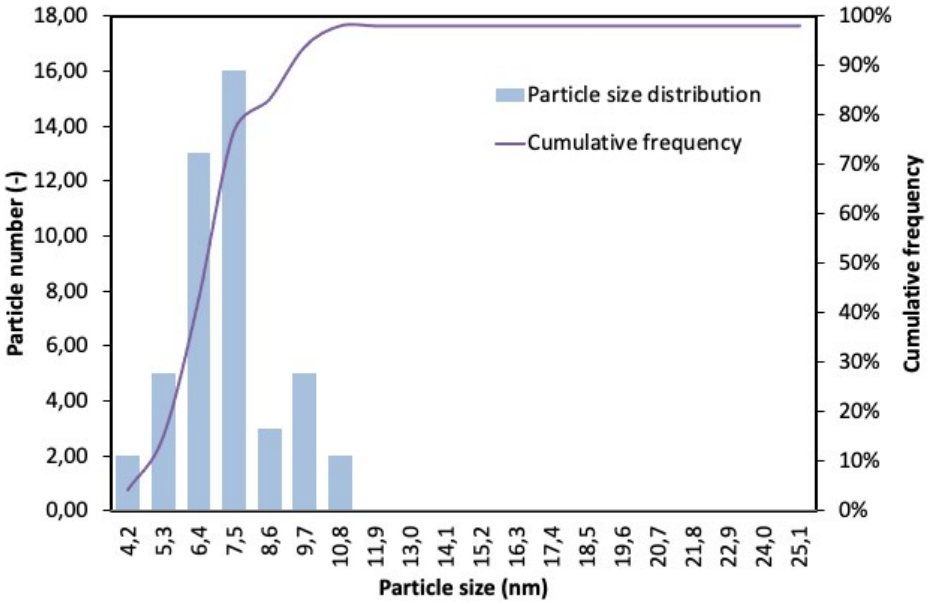

Fig. S6: Size distribution of commercial TiO_2 nanoparticles used in paint

The particles size distribution was based on the determination of the minimum Feret diameter of 7.05 nm particles base on 46 particles obtained by SEM, Hitachi S-5500, Japan.

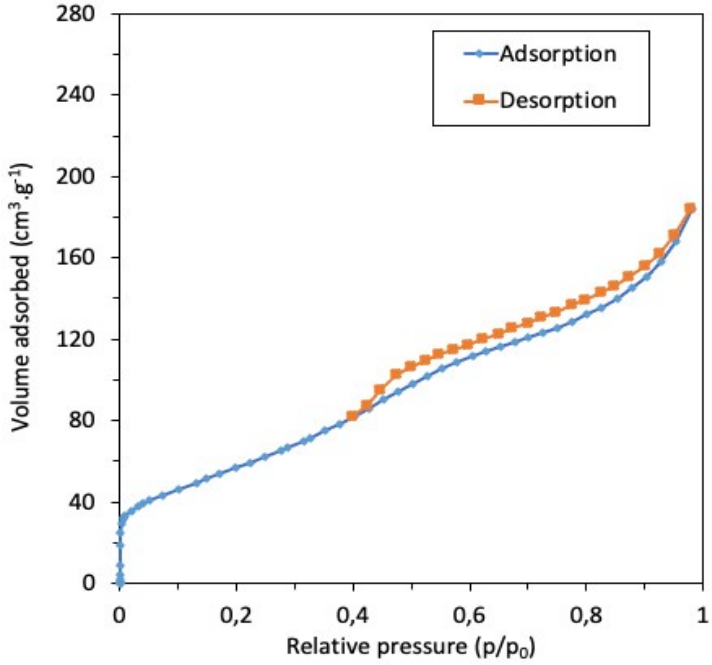

Fig. S7: N_2 adsorption-desorption isotherms at 77 K of commercial TiO_2 nanoparticles used in paint. Sample was previously outgassed at 400 °C during 1000 minutes under secondary vacuum

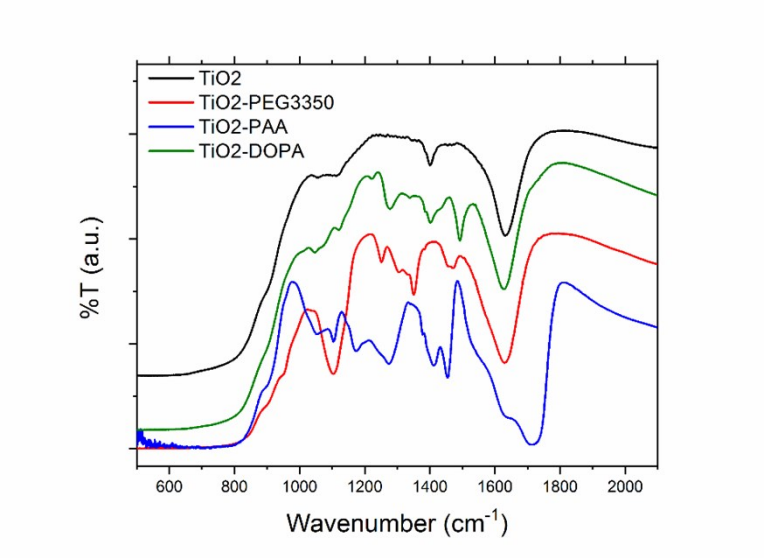

Fig. S8: FTIR spectra (KBr pellet) of the pristine commercial TiO_2 NPs (in black) and the commercial TiO_2 NPs coated with PEG3350 (in red), PAA (in blue) and DOPA (in green)

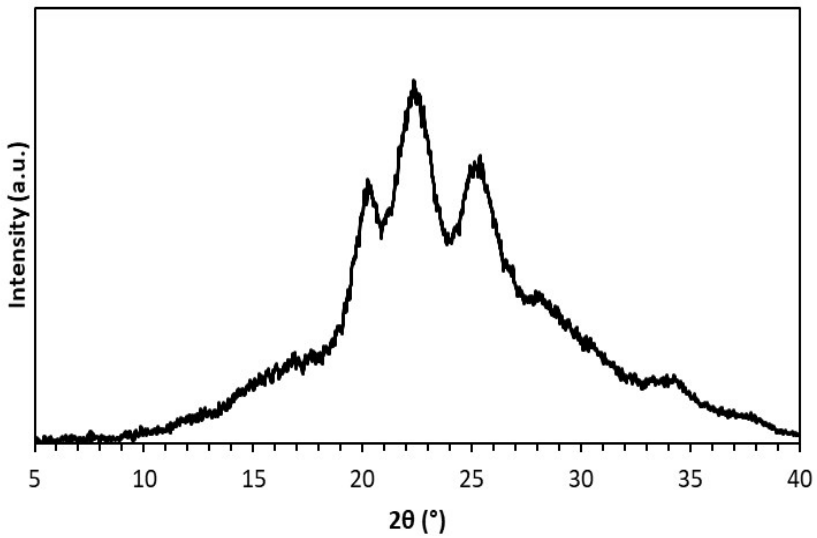

Fig. S9: XRD diffractogram of the TiO_2-CNC hybrids, with the peak at 25° characteristic of anatase TiO_2

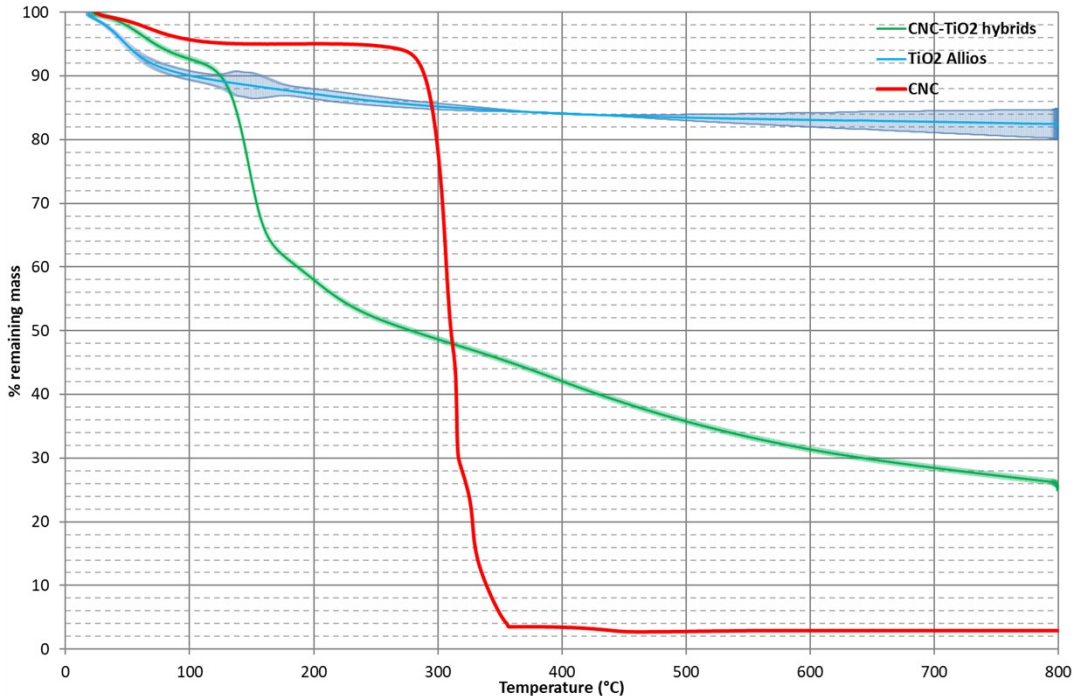

Fig. S10: TGA thermograms of the initial CNC (in red), of the pristine commercial TiO_2 NPs (in blue) and of the CNC-TiO_2 hybrids (in green)

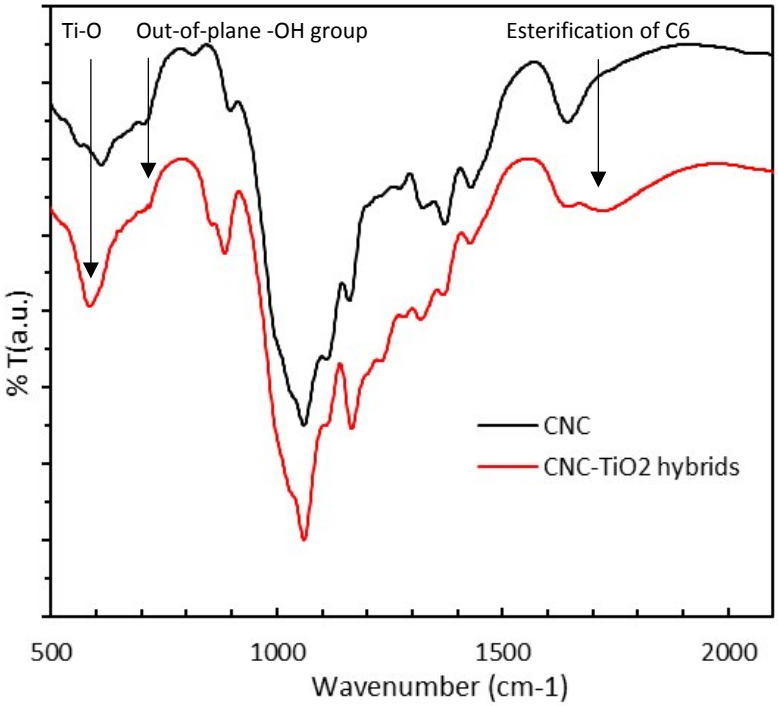

Fig. S11: FTIR spectra (KBr pellet) of the initial CNC (in black) and of the CNC-TiO_2 hybrids (in red)

The FTIR spectra show that the TiO_2 was grafted onto CNC. The peak at 580 cm^{-1} was identified to Ti-O bonds in the TiO_2 lattice. The peak at 1720 cm^{-1} corresponds to the esterification of out-of-plane hydroxyl groups located on C6 of the glucose molecule. The peak at 710 cm^{-1} corresponds to out-of-plane hydroxyl group bending at C6 of the glucose molecule. This peak disappears when the CNC is grafted with TiO_2. It is the esterification of C6, which replaces the out-of-plane hydroxyl group with Ti.[1]

Table S*1*: Chemical composition of reference paint P2 analyzed by XPS before and after artificial weathering

Reference paint	Artificial weathering (hours)	C 1s (%.at)	O 1s (%.at)	Ca 2p (%.at)	Ti 2p (%.at)
P2	0	82.4	9.7	3.6	1.8
	500	27.4	38.3	1.9	22.8
	1000	30.5	36.7	1.5	22.1

Table S*2*: Chemical composition of paint P3 analyzed by XPS before and after artificial weathering

Paint	Artificial weathering (hours)	C 1s (%.at)	O 1s (%.at)	Ca 2p (%.at)	Ti 2p (%.at)
P3	0	73.7	15.0	4.2	2.0
	500	76.0	12.5	4.3	3.3
	1000	27.3	37.5	1.5	21.2

Table S*3*: Chemical composition of paint P6 analyzed by XPS before and after artificial weathering

Paint	Artificial weathering (hours)	C 1s (%.at)	O 1s (%.at)	Ca 2p (%.at)	Ti 2p (%.at)
P6	0	80.7	9.4	1.2	2.7
	500	73.6	16.0	5.5	1.0
	1000	56.0	17.5	1.3	9.5

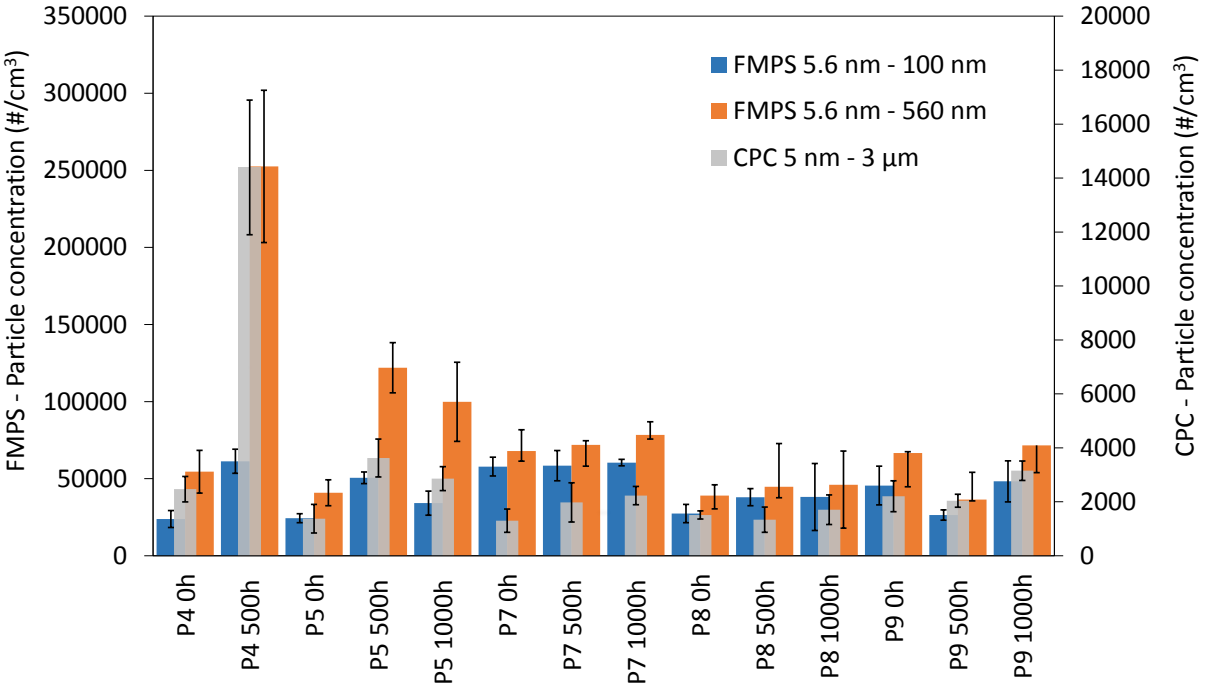

Fig. S12: Concentration of particles released per cm³ before and after artificial weathering as a function of the particle size measured with FMPS (left scale) in blue from 5.6 nm to 100 nm and in orange from 5.6 nm to 560 nm and CPC (right scale) in grey from 5 nm to 3 µm

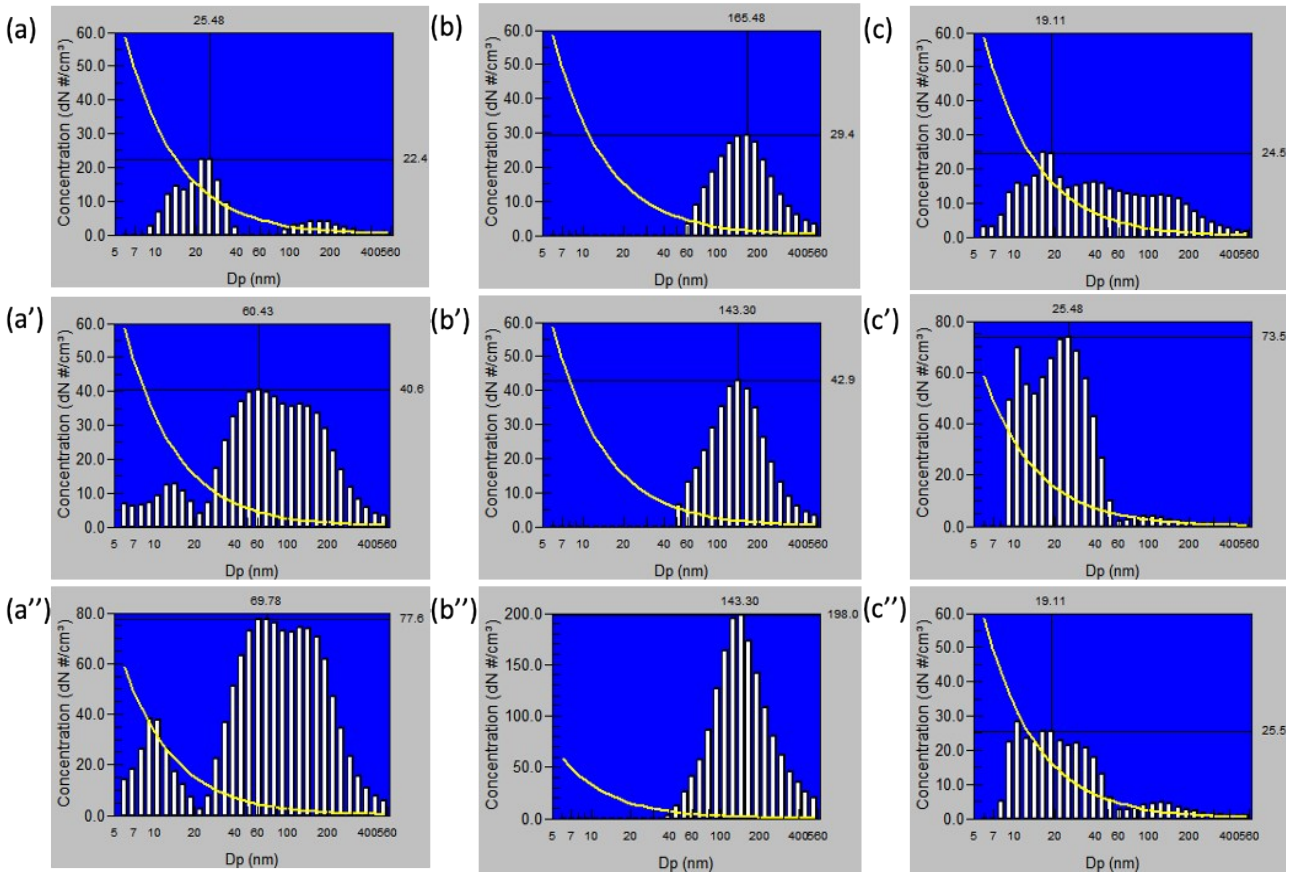

Fig. S13: Particle size distribution of particles released from paints P2, P3 and P6 respectively before artificial weathering (a), (b) and (c), after 500 hours exposure (a'), (b') and (c') and after 1000 hours exposure (a''), (b'') and (c'') measured by a fast mobility particle sizer (FMPS)

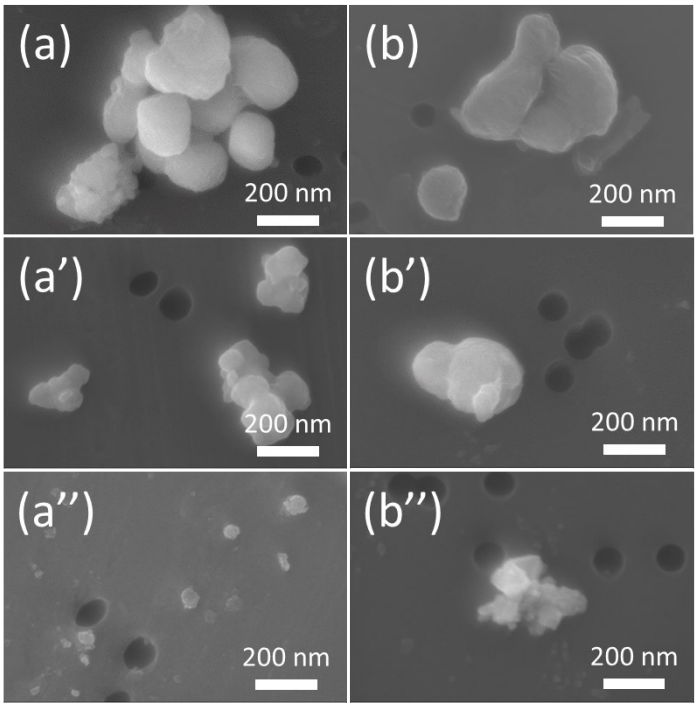

Fig. S14: SEM images of submicromic agglomerates, individual submicronic particles and individual nanoparticles released from paints P3 (a) and P6 (b). The paints after 500 hours and 1000 hours exposure to artificial weathering are noted respectively with (') and ('')

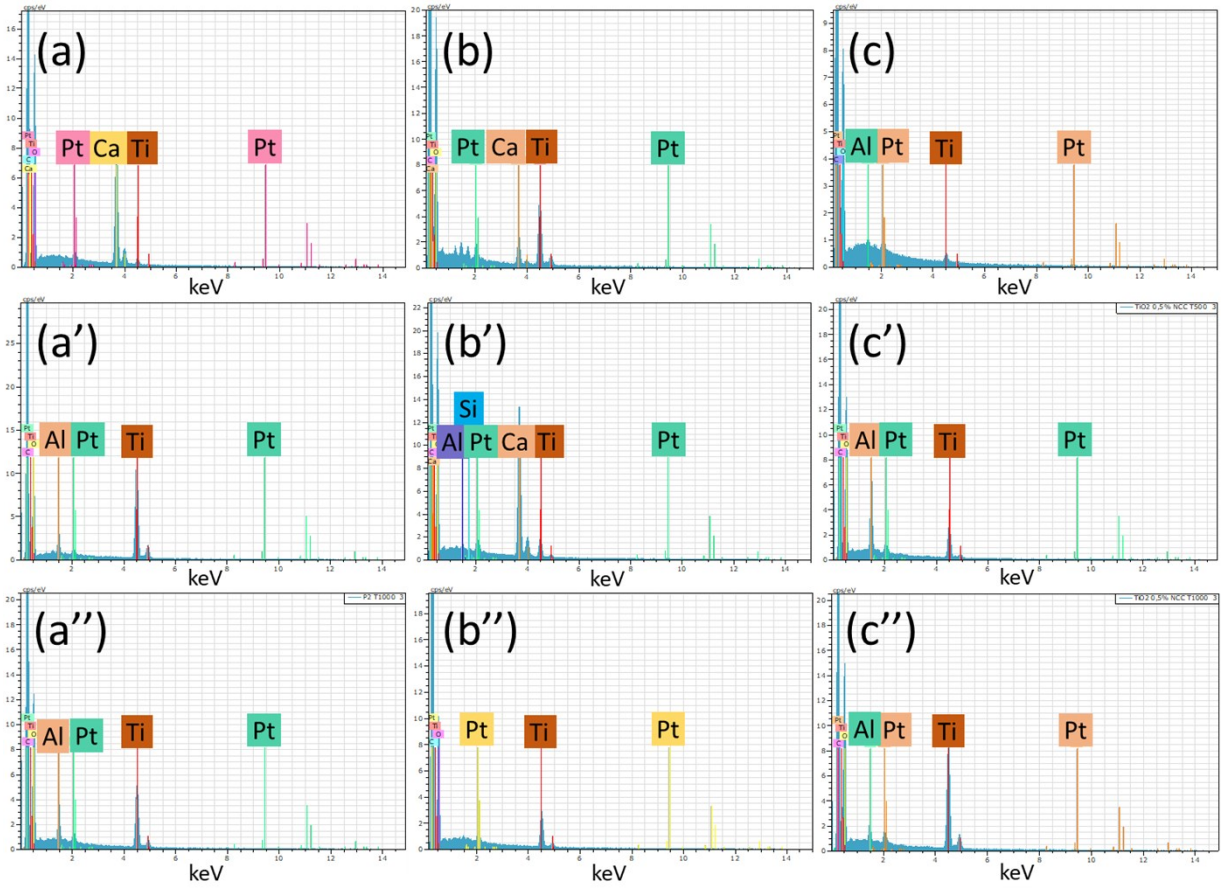

Fig. S15: EDX spectra of particles released from paints P2, P3 and P6 respectively before artificial weathering (a), (b) and (c), after 500 hours exposure (a'), (b') and (c') and after 1000 hours exposure (a''), (b'') and (c'')

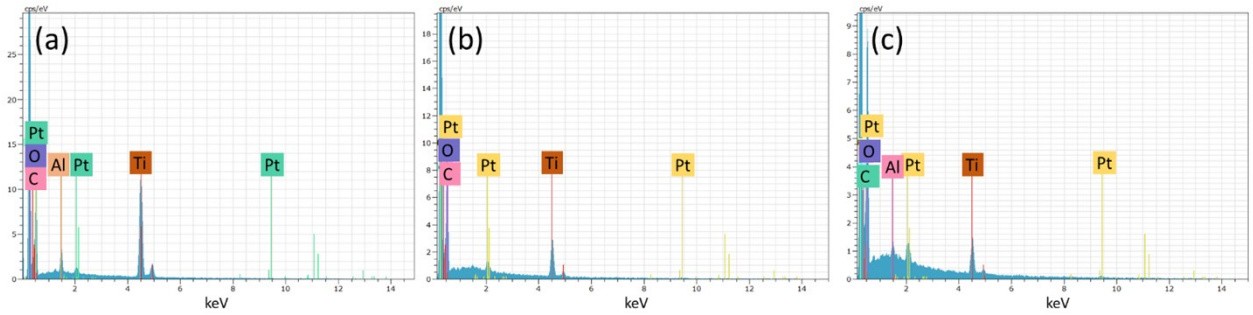

Fig. S16: EDX spectra of individual submicronic particles and individual nanoparticles released from paints P2 (a), P3 (b) and P6 (c)

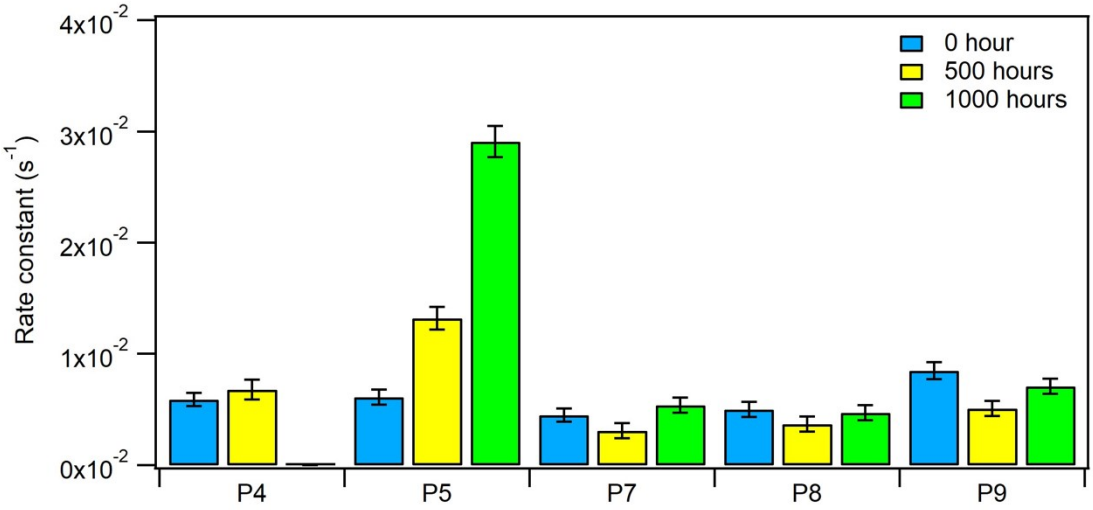

Fig. S17: *m*-xylene kinetic constant as a function of the paints P4, P5, P7, P8 and P9 before and after artificial weathering 500 hours and 1000 hours. The errors bars are derived from uncertainties associated to experiments

Table S4: *m*-xylene kinetic constant for the paints before and after artificial weathering 500 hours and 1000 hours

Paints	k (s^{-1}) 0 hour	k (s^{-1}) 500 hours	k (s^{-1}) 1000 hours
P2	$4.8 \cdot 10^{-3} \pm 0.6 \cdot 10^{-3}$	$1.53 \cdot 10^{-2} \pm 0.10 \cdot 10^{-2}$	$1.55 \cdot 10^{-2} \pm 0.10 \cdot 10^{-2}$
P3	$6.5 \cdot 10^{-3} \pm 0.7 \cdot 10^{-3}$	$2.24 \cdot 10^{-2} \pm 0.11 \cdot 10^{-2}$	$4.16 \cdot 10^{-2} \pm 0.18 \cdot 10^{-2}$
P4	$5.9 \cdot 10^{-3} \pm 0.6 \cdot 10^{-3}$	$0.68 \cdot 10^{-2} \pm 0.09 \cdot 10^{-2}$	-
P5	$6.1 \cdot 10^{-3} \pm 0.7 \cdot 10^{-3}$	$1.32 \cdot 10^{-2} \pm 0.10 \cdot 10^{-2}$	$2.91 \cdot 10^{-2} \pm 0.14 \cdot 10^{-2}$
P6	$4.3 \cdot 10^{-3} \pm 0.6 \cdot 10^{-3}$	$0.39 \cdot 10^{-2} \pm 0.07 \cdot 10^{-2}$	$0.82 \cdot 10^{-2} \pm 0.07 \cdot 10^{-2}$
P7	$4.5 \cdot 10^{-3} \pm 0.6 \cdot 10^{-3}$	$0.31 \cdot 10^{-2} \pm 0.07 \cdot 10^{-2}$	$0.54 \cdot 10^{-2} \pm 0.07 \cdot 10^{-2}$
P8	$5.0 \cdot 10^{-3} \pm 0.7 \cdot 10^{-3}$	$0.37.10^{-2} \pm 0.07 \cdot 10^{-2}$	$0.47 \cdot 10^{-2} \pm 0.07 \cdot 10^{-2}$
P9	$8.5 \cdot 10^{-3} \pm 0.7 \cdot 10^{-3}$	$0.51.10^{-2} \pm 0.07 \cdot 10^{-2}$	$0.71 \cdot 10^{-2} \pm 0.07 \cdot 10^{-2}$

Table S5: Removal efficiency of m-xylene in position A_4 for photocatalytic paints P4, P5 and P7-P9 before and after artificial weathering 500 hours and 1000 hours

Paints	RE 0 hour (%)	RE 500 hours (%)	RE 1000 hours (%)
P4	14.6	26.4	NA
P5	15.1	35.1	53.5
P7	13.9	15.9	18.4
P8	19.1	13.0	16.4
P9	17.0	17.2	20.2

Reference

1 N. Shandilya and I. Capron, *RSC Adv.*, 2017, **7**, 20430–20439.